Materials Science-Poland, 35(3), 2017, pp. 660-666
http://www.materialsscience.pwr.wroc.pl/
DOI: 10.1515/msp-2017-0072

DE GRUYTER OPEN

Synthesis of Pd–Ni/C bimetallic materials and their application in non-enzymatic hydrogen peroxide detection

HILAL CELIK KAZICI*, FIRAT SALMAN, HILAL DEMIR KIVRAK

Yüzüncü Yıl University, Institute of Science, Department of Chemical Engineering, Van, Turkey

In this study, carbon based bimetallic materials (Pd–Ni/C) were synthesized by polyol method in order to increase the hydrogen peroxide reduction catalytic activity of Pd using Ni metal. Hydrogen peroxide reduction and sensing properties of the prepared catalysts were measured by electrochemical methods. As a result, we have established that the addition of Ni at different ratios to Pd has a considerable electrocatalytic effect on H_2O_2 reduction. This work provides a simple route for preparation of Pd–Ni catalysts to create a very active and sensible electrochemical sensor for H_2O_2 sensing.

Keywords: *bimetallic structure; hydrogen peroxide sensor; polyol; catalyst*

1. Introduction

Hydrogen peroxide (H_2O_2) is a typical peroxide, commonly found in nature, which is widely used in food production, chemical synthesis, fuel cells, and pharmaceutical analysis [1–3]. In addition, H_2O_2 is the major predictor of oxidative stress, and at the same time, it is very reactive and capable of forming detrimental hydroxyl radicals [4–6].

Thus, the preparation of variable and correct sensing process for precise monitoring of H_2O_2 has been investigated at a comprehensive level. There are several techniques for determination of H_2O_2, such as colorimetric assay, electrochemiluminescence and electrochemistry [7–10].

Electrochemistry is the most convenient method for H_2O_2 determination due to the low limits of detection, high selectivity, and sensibility [11, 12]. However, it often suffers from low stability as well as low reusability because of the internal structure of enzymes. Enzyme-free methods help to remove the disadvantages of the enzymatic processes. H_2O_2 can rapidly be electrochemically measured by direct reduction or oxidation method [13].

Metal nanoparticles have many unique properties such as large surface-to-volume ratio, high surface reaction activity, high catalytic efficiency, and strong adsorption ability [14].

Bimetallic NPs have higher catalytic activity and better selectivity than their monometallic equivalents since they have strong synergistic effect between metals. In addition, different bimetal nanostructures have been described by Wang et al. [12] and they have shown that these NPs present significant catalytic performance.

However, addition of other transition metals to Pd may improve its electrochemical efficiency by altering the electronic structure. Pure nickel (Ni) is ductile and tough because it has a face-centered cubic (fcc) crystal structure up to its melting point and shows a remarkable synergistic effect of increasing the electrochemical efficiency of Pd [15].

Especially, the efficiency of metal nanoparticles used as a catalyst is directly related to the synthesis method. Traditional preparation methods such as sol-gel, microemulsion, co-precipitation, and chemical vapor deposition could have been used, however, alternative methods have been developed [16–19].

Polyol synthesis is one of the methods preferred for synthesizing metal-based catalysts, and it can be a good alternative for solution of existing

*E-mail: hcelik@eng.ankara.edu.tr

problems such as sintering, coking, phase change, and deactivation. This synthesis method, which provides nanosized particles, is an economical and simple process. Since the reduction processes are carried out in solutions, an extra processing is not required, so the formation and growth steps could be controlled [20, 21].

The base material can affect the catalytic activity of catalysts. Carbon-based catalysts are commonly used in catalytic reactions [22]. An effective catalyst base material has a large surface area that provides complete active sites for metal nanoparticles that have catalytic properties. In addition, for diffusion and adsorption purposes, a relatively large pore size is required at the mesoscale in most applications [23, 24].

Some electrochemical sensor processes have been reported using noble metal nanoparticles [25–28]. For example, Li et al. [29] prepared a non-enzymatic H_2O_2 sensor based on Au–Ag nanotubes and chitosan film. Kivrak et al. [30] successfully synthesized carbon-based Pt–MnOx, and Pt nanoparticles have been proposed for sensing of hydrogen peroxide (H_2O_2) in a new electrochemical sensor using a microwave irradiation method. Shen-Ming et al. [31] reported that silver nanowires (AgNWs) are very responsive amperometric H_2O_2 sensors attached to the modified screen printed carbon electrode (SPCE) using the polyol method. Zhao et al. [32] prepared nanoporous palladium-nickel alloy with very sensitive to hydrogen peroxide and glucose.

The aim of this work is to report the synthesis of the Pd and (Pd–Ni/C) bimetallic nanoparticles using ethylene glycol (EG) and its application as an H_2O_2 sensor. The morphology, size, structure, and composition of the resultant bimetallic nanoparticles have been characterized by scanning electron microscopy (SEM), X-ray diffraction (XRD), and energy-dispersive X-ray spectroscopy (EDX).

Even though many studies were performed on carbon based polyol synthesis and application of this compound as an H_2O_2 sensor, none of them have systematically studied the relationship between the size of nanoparticles and applications using the technique reported herein.

2. Experimental

2.1. Apparatus

Voltammetric measurements were carried out using CHI 660E Electrochemical Analyzer with a three-electrode system consisted of a working electrode (bare GCE, Nafion/GCE, Pd–Ni–NGCE), a platinum wire counter electrode, and an Ag/AgCl (sat. KCl) reference electrode, respectively. Cyclic voltammetry (CV) and chronoamperometric (CA) measurements were used during the electroanalytical studies. The pH measurements were performed with Autolab analyzer pH-meter. Magnetic stirrer model was Isolab.

2.2. Reagents and materials

All reagents were of analytical reagent grade. Hydrogen peroxide (H_2O_2) (Aldrich) and ethylene glycol (EG) (Aldrich, 99.5 %) were used as received. Nickel sulfate ($NiSO_4$), sodium dihydrogen phosphate (NaH_2PO_4), disodium monohydrogen phosphate (Na_2HPO_4), and ethanol (C_2H_5OH) were supplied from Merck. Buffer solutions were made from sodium dihydrogen phosphate/disodium monohydrogen phosphate (PBS) with pH = 7.5. Palladium solution was prepared by dissolving 0.01 g (1.0×10^{-3} mol·L^{-1}) $PdSO_4$ in 100.0 mL 0.1 mol·L^{-1} H_2SO_4 solution. Nickel solution was prepared by dissolving 0.07 g $NiSO_4$ (1.0×10^{-3} mol·L^{-1}) in 250.0 mL 0.1 mol·L^{-1} H_2SO_4 solution. Our solutions were prepared and diluted with ultrapure water (Millipore Milli Q system, 18.2 MΩ).

2.3. Preparation of electrode

GCE was activated by polishing with Al_2O_3 slurry (0.05 μm to 3 μm), then rinsed with distilled water and ultrasonically treated for 3 min in ethanol solution (1:1 v/v) mixture. GCE was also electrochemically cleaned by keeping for 10 min at a constant potential of 1.0 V. To prepare the electrode, 5 mg of the catalyst was stirred in 1 mL of 5 % nafion solution to obtain the catalyst ink.

Subsequently, 5 μL of the ink was deposited on the surface of the glassy carbon electrode. The electrode was dried at room temperature to remove the solvent.

2.4. Preparation of Pd–Ni/C nanoparticles

Carbon based Pd and Pd–Ni catalysts were prepared by polyol method. To examine the effect of Ni addition on the reduction of hydrogen peroxide, the carbon based Pd–Ni catalysts were prepared at different Pd:Ni atomic ratios (9:1, 7:3, 5:5). Then, the non-enzymatic hydrogen peroxide (H_2O_2) sensing activities of these catalysts were measured by electrochemical techniques.

Firstly, Pd metal salt and carbon were dissolved in ethylene glycol; the pH of this solution was set to 7.5 to prepare catalyst Pd–M (M = Ni) nanoparticles. Thereafter, the temperature was increased to 130 °C and the mixture was kept at this temperature by refluxing in an oil bath for 2 h. After the refluxing, the slurry suspension was rapidly cooled down in cold water, filtered, and dried in a vacuum oven at 70 °C for 4 hours. As a result, powder from the catalyst was obtained. Pd metal loading per gram carbon was 10 % for all the catalysts. For the preparation of the monometallic catalyst, the same process was followed.

2.5. Characterization

Scanning electron microscopy (SEM) and energy dispersive X-ray (EDX) spectroscopy studies were carried out using an FEI QUANTA 250 FEG scanning electron microscope. X-ray diffraction setup, Rigaku RadB-DMAX II with CuKα radiation (λ = 1.54056 Å) was used to perform XRD measurements. The samples were prepared by depositing carbon-based modified nanoparticles on a glass surface and then drying in a vacuum oven.

3. Results and discussion

3.1. X-Ray diffraction (XRD) characterization of the Pd–Ni/C catalysts

Crystallographic information of Pd/C and Pd–Ni/CNT catalysts was obtained from XRD measurements. The diffraction patterns show that the structure can be indexed using Pd face centered-cubic (fcc) lattice, with (1 1 1), (2 0 0), and (2 2 0) crystal planes. For the Pd–Ni/C nanocatalyst, the XRD profile and the peaks are shifted towards higher 2θ angles associated with the (1 1 1), (2 0 0), and (2 2 0) planes at 2θ values of 39.6°, 42.6°, and 64.4°. The broad peak around 24° for all materials corresponds to the (0 0 2) plane of carbon phase (Fig. 1). Correlation of the effects caused by different second metals, is a further argument in favor of the concept of bimetallic structures which take advantages from the both metals.

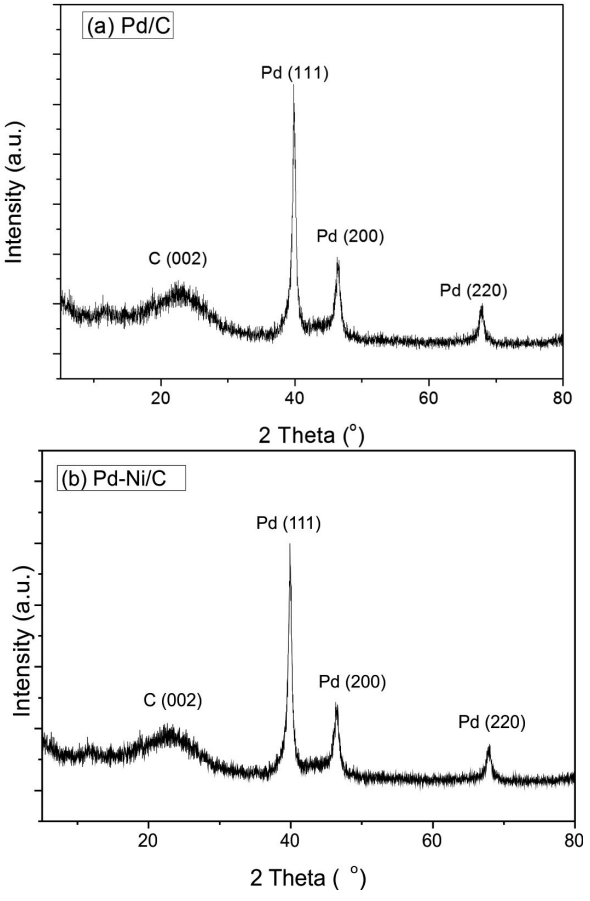

Fig. 1. XRD patterns of (a) Pd/C, (b) Pd–Ni/C catalysts.

3.2. SEM-EDX measurements

SEM images of Pd/C and Pd–Ni/C electrodes are presented in Fig. 2 and the EDX spectrum for Pd–Ni/C is shown in Fig. 2c. It

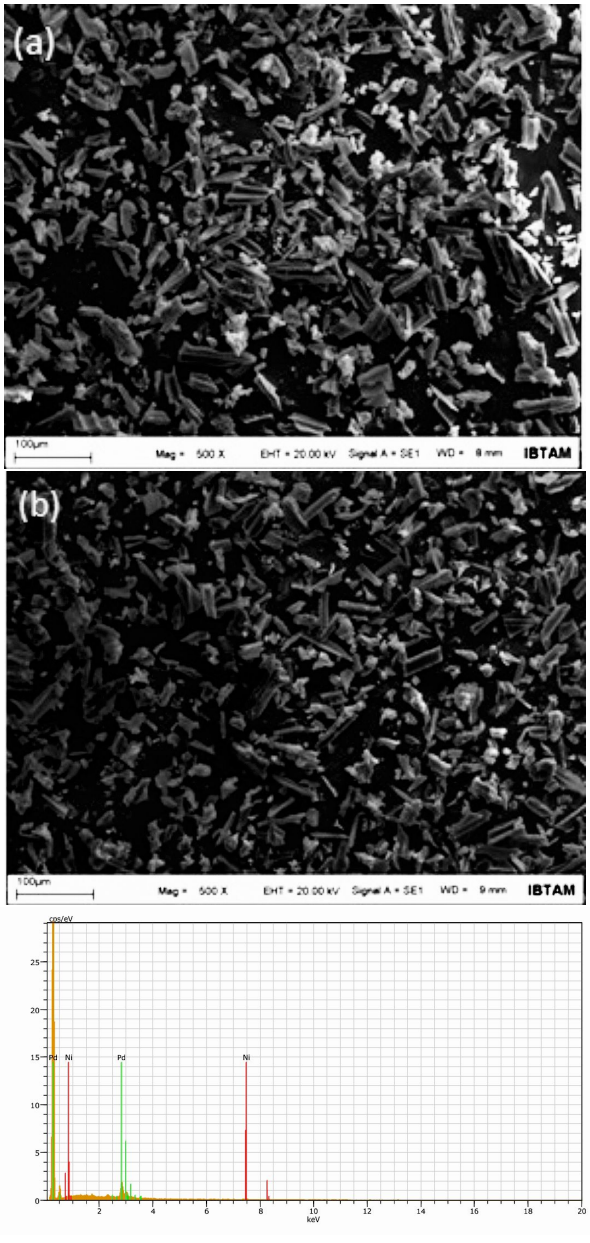

(c)

Fig. 2. SEM images of (a) Pd/C, (b) Pd–Ni/C and (c) EDX spectrum of Pd–Ni/C catalysts.

is seen that the Pd/C sample has a rougher surface with larger particles compared to Pd–Ni/C catalyst. For the Pd–Ni/C catalyst, EDX analysis reveals the presence of Pd and Ni. According to EDX results (Fig. 2c), Pd–Ni/C catalyst has 70.30:29.70 Pd:Ni atomic ratio, which is in a good agreement with the stoichiometric ratio (70: 30) used in the preparation procedure.

3.3. Electrochemical behavior of H_2O_2 over the Pd–Ni/C

The electrocatalytic activity of the obtained Pd-Ni nanoparticles towards H_2O_2 was evaluated by cyclic voltammetry (CV). Primarily, CV measurements were taken in 0.1 M phosphate buffer solution with a scan rate of 100 $mV \cdot s^{-1}$ on Pd/C and Pd–Ni/C electrodes (Fig. 3). H_2O_2 measurements were performed at 1 mM concentration of the Pd/C (1:0) and Pd_7–Ni_3/C catalysts (Fig. 3a).

Fig. 3a shows the cyclic voltammetry graph (CVs) of the bare as well as modified electrodes in PBS solution in either presence or absence of H_2O_2. The current density for H_2O_2 reduction on Pd–Ni/C in the range of –0.25 V to 0.5 V is more than 2 times higher than for Pd/C. The improved electrochemical activity of Pd–Ni core/shell toward H_2O_2 may also result from the synergistic effects between Pd and Ni atoms besides the nanoporous materials.

During this research, different atomic ratios have also been tested. Pd–Ni/C electrocatalysts with three different (9:1, 7:3, and 5:5) atomic ratios were synthesized. The cyclic voltammetry experiments of each catalyst were carried out under the same conditions as the previous experiments. The voltammetry curves obtained for each atomic ratio are shown in Fig. 3b.

In this study, it was found that especially Pd_{70}–Ni_{30}/C showed the best electronic coupling effect due to the best catalytic properties.

Electrochemical sensing properties of Pd_7–Ni_3/C towards H_2O_2 were qualitatively studied by cyclic voltammetry measurements with successive increment of H_2O_2 (0 mM and 1 mM) in 20 mL 0.1 M PBS (pH 7.5, 25 °C) at a scan rate of 0.01 $mV \cdot s^{-1}$ (Fig. 3c). The reduction peak current of Pd_7–Ni_3 / C at 0.5 V increases significantly upon successive addition of H_2O_2. This result clearly states that the modified electrode has a high electrocatalytic performance towards H_2O_2 and thus Pd_7–Ni_3/C can be used as a H_2O_2 sensor. The electrochemical behavior of Pd_7–Ni_3/C towards H_2O_2 reduction was further explored by changing the scan rate (Fig. 3d).

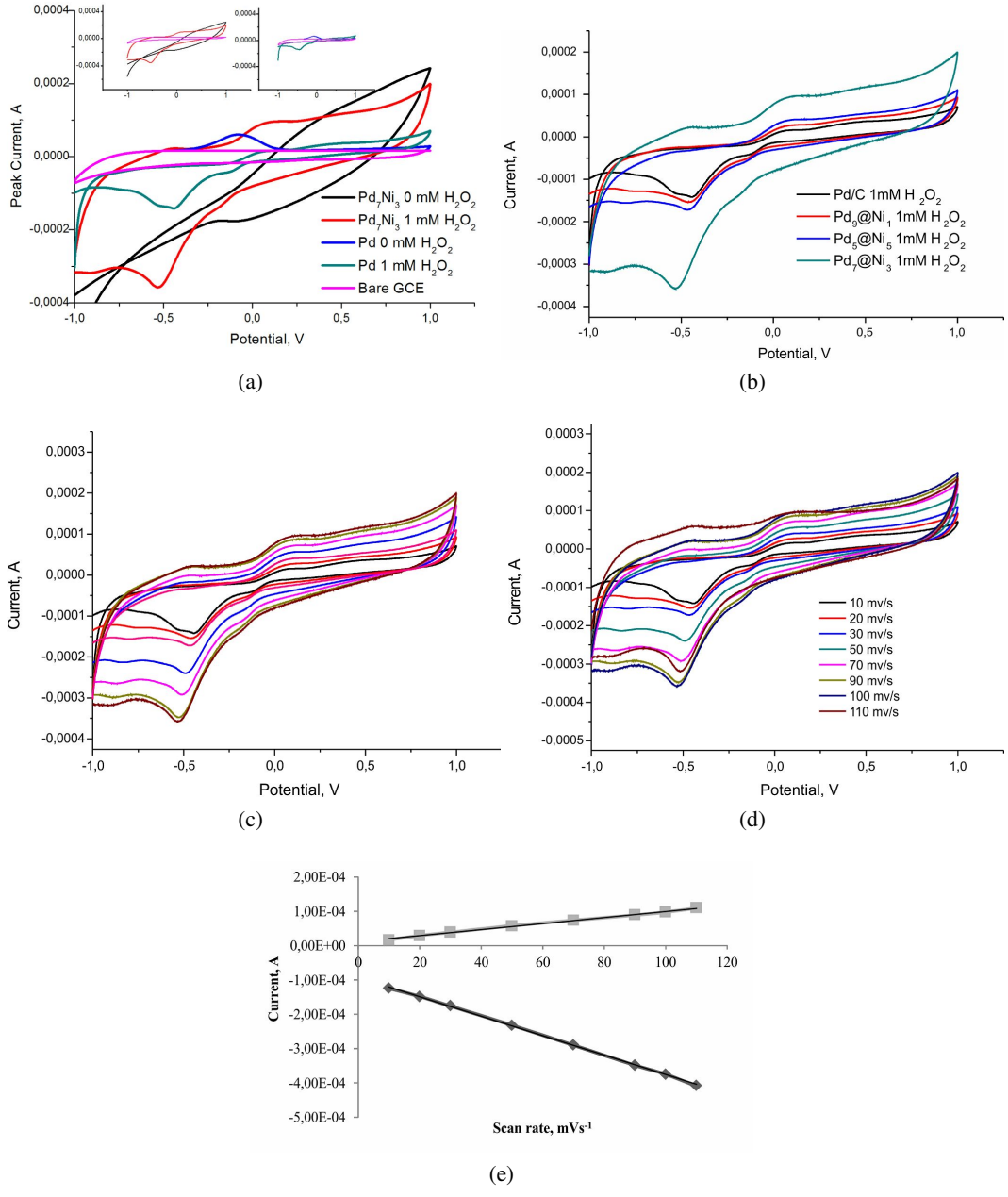

Fig. 3. CVs of (a) bare GCE, Pd/C (1:0), Pd_7–Ni_3/C in PBS solution in the presence of H_2O_2 and Pd/C (1:0), Pd_7–Ni_3/C in PBS solution in the absence of H_2O_2 (b) Pd/C (1:0), Pd–Ni/C (7:3, 5:5, 9:1) (c) Pd_7–Ni_3/C in 0.1 M PBS (pH 7.5) including different amounts of H_2O_2 (0, 0.3, 0.5, 0.7, 0.8, 0.9 and 1 mM) (d) Pd_7–Ni_3/C in PBS + 1 mM H_2O_2 solution at different scan rates of 10 mV/s, 20 mV/s, 30 mV/s, 50 mV/s, 60 mV/s, 70 mV/s, 80 mV/s, 90 mV/s, 100 mV/s and 110 mV/s. (e) Plots of current on Pd_7–Ni_3/C at 0.1 V.

It is understandable that as the scan rate increases, the peak-to-peak decomposition widens. Peak currents of reduction and oxidation rise linearly with increasing the value of scan rate. Correlation coefficients for anodic and cathodic peaks are 0.997 and 0.999, respectively. It is also observed that the electrochemical kinetic reaction is surface controlled (Fig. 3e).

Table 1. Comparison of performances of different electrodes of sensors used for determination of H_2O_2.

Electrodes	Linear range [mM]	Detection limit [mM]	The literature
NP–PdNi	0.05 –1.0	0.0021	[38]
MWCNTs-Pd	1 – 10	0.0003	[40]
PDDA/t-MWCNT-Pt/GCE	0.001 – 8	0.00027	[41]
Ag/MWCNT	0.1 – 0.9	0.0022	[42]
Graphene/MWCNT	0.0002 – 2.1	0.0094	[43]
Graphene oxide/GC	0.001 – 0.016	0.007	[44]
Pd–Ni/C	0.0003 – 1	0.000062	This work

Due to the high electro-reduction activity towards H_2O_2, the detection performance of Pd_7–Ni_3/C was assessed by amperometric sensing upon further addition of H_2O_2.

Fig. 4a shows the characteristic amperometric responses of Pd_7–Ni_3/C at a constant potential. It is seen that Pd_7–Ni_3/C electrode responds quickly (∼1 s) to each addition of H_2O_2.

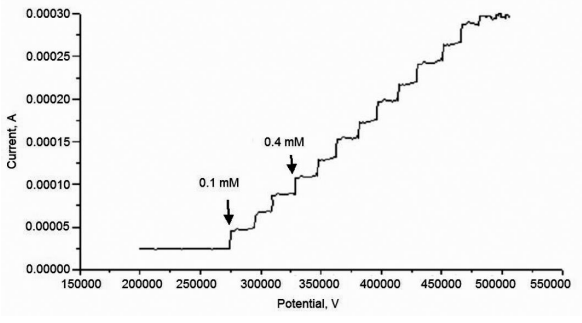

(a)

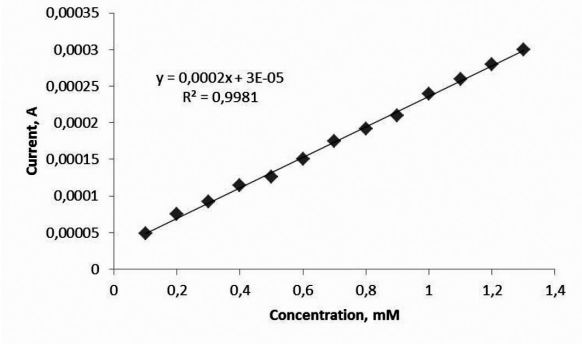

(b)

Fig. 4. (a) Amperometric response of Pd_7–Ni_3/C on adding of 0.1 mM H_2O_2 into PBS solution at 0.2 V (b) Plot of current vs. H_2O_2 concentration.

The relation between the current and H_2O_2 concentration is as follows:

$$i(\mu A) = 0.0002C_{H_2O_2} + 3 \times 10^{-5}, R^2 = 0.9981 \quad (1)$$

where i is the peak current and C is the concentration of H_2O_2. To evaluate LOD (limit of detection), we fitted the straight lines obtained from equation 2 to the data in Fig. 4b, and applied the widely used criterion for LOD [33].

The LOD and LOQ (limit of quantification) were obtained as 6.2×10^{-5} mmol·L^{-1} and 1.98×10^{-4} mmol·L^{-1} H_2O_2, respectively, using the relation LOD = $3 \times S_{y/x}/m$ and LOQ = $10 \times S_{y/x}/m$, where m is the slope of the first calibration plot and $S_{y/x}$ is the standard error of estimate of the calibration curve (equation 2):

$$S_{y/x} = \sqrt{\frac{\sum_{i=1}^{N}(yi - \hat{y})^2}{N-2}} \quad (2)$$

where yi is the measured signal, $\hat{y}$ is the concentration measured for this signal, and N is the number of points in the calibration graph.

The parameters of Pd_7–Ni_3/C obtained from this analysis are better than the parameters of other catalysts used in H_2O_2 sensors, shown in Table 1. The significant performance of the Pd_7–Ni_3/C modified electrode towards the H_2O_2 detection shows that Pd_7–Ni_3/C has a great potential for fabrication of H_2O_2 sensors.

4. Conclusions

Pd_7–Ni_3/C nanoparticles were successfully synthesized and characterized by SEM, XRD, EDX, and cyclic voltammetry. The results showed that Pd_7–Ni_3/C nanoparticles had excellent catalytic activity in H_2O_2 reduction. When the optimum running potential of the sensor was 0.2 V, the best sensitivity was achieved with the Pd_7–Ni_3/C due to the optimum electronic coupling effect at the deposition potential of -0.5 V for 10 min. The chronoamperometric measurements showed that the peak current for H_2O_2 rose linearly with its concentration in the range of 0.0003 mM to 1 mM (detection limit was 0.000062 mM). Pd_7–Ni_3/C nanoparticles can be the leading material for commercial disposable H_2O_2 sensors due to high sensitivity, easy production, and low-cost.

Acknowledgements

This study was supported by the Scientic and Technological Research Council of Turkey (TUBİTAK) in terms of finance with the Project No. 1919B011403555.

References

[1] HAN Y., ZHENG J., DONG S., *Electrochim. Acta*, 90 (2013), 35.
[2] SITNIKOVA N.A., BORISOVA A.V., KOMKOVA M.A., KARYAKIN A.A., *Anal. Chem*., 83 (2011), 2359.
[3] SANG Y., ZHANG L., LI Y.F., CHEN L.Q., XU J.L., HUANG C.Z., *Anal. Chim. Acta*., 659 (2010), 224.
[4] GEISZT M., LETO T.L., *J. Biol. Chem*., 279 (2004), 51715.
[5] GIORGIO M., TRINEI M., MIGLIACCIO E., PELICCI P.G., *Nat. Rev. Mol. Cell Biol*., 8 (2007), 722.
[6] LALOI C., APEL K., DANON A., *Curr. Opin. Plant Biol*., 7 (2004), 323.
[7] WEN T., QU F., LI N.B., LUO H.Q., *Anal. Chim. Acta*, 749 (2012), 56.
[8] CHENG Y.F., YUAN R., CHAI Y.Q., NIU H., CAO Y.L., LIU H.J., BAI L.J., YUAN Y.L., *Anal. Chim. Acta*, 745 (2012), 137.
[9] ABO M., URANO Y., HANAOKA K., TERAI T., KOMATSU T., NAGANO T., *Am. J. Chem. Soc*., 133 (2011), 10629.
[10] ANJUM S., LIU Z., GAO W., QI W., REHAN H.S.G.M., AHMAD M., REHMAN A., XU G., *J. El. Chem*., 750 (2015), 74.
[11] KAFI A.K.M., WU G., CHEN A., *Biosens. Bioelectron*., 24, (2008), 566.
[12] WANG B., ZHANG J.J., PAN Z.Y., TAO X.Q., WANG H.S., *Biosens. Bioelectron.*, 24 (2009), 1141.
[13] CHAKRABORTY S., RETNA C.R., *Biosens. Bioelectron.*, 24 (2009), 3264.
[14] YUANYUANG L., HERMANN J. S., SHUNQING X., *Gold Bull.*, 43 (2010), 29.
[15] ZHAO D.Y., WANG Z.H., WANG J.P., XU C.X., *J. Mater. Chem. B*., 2 (2014), 5195.
[16] TANG S., JI L., LIN J., ZENG H.C., TAN K.L., LI K., *J. Catal*., 194 (2000), 424.
[17] SHIRAZ M.H.A., REZAEI M., MESHKANI F., *Int. J. Hydrogen Energ.*, 41 (2016), 6353.
[18] LIUA J., SUNA B., HUA J., PEIA Y., LIB H., QIAO M., *J. Catal.*, 274 (2010), 287.
[19] MOSHKALYOV S.A., MOREAU A.L.D., GUTTIÉRREZ H.R., COTTA M.A., SWART J.W., *Mater. Sci. Eng. B-Adv*., 112 (2000), 147.
[20] YING Z., SHENGMING J., GUANZHOU Q., MIN Y., *Mater. Sci. Eng. B-Adv.*, 122 (2005), 222.
[21] PARK B.K., JEONG S., KIM D., MOON J., LIM S., KIM J.S., *J. Colloid Interf. Sci*., 311 (2007), 417.
[22] YU K., KIM D.J., CHUNG H.S., LIANG H., *Mater. Lett.*, 57 (2003), 3992.
[23] CANDELARIA S.L., GARCIA B.B., LIU D., CAO G., *J. Mater. Chem. Mater*., 22 (2012), 9884.
[24] WU Z., KONG L., HU H., TIAN S., XIONG Y., *ACS Sustain. Chem. Eng*., 3 (2015), 552.
[25] ZHANG J., SHI Q., ZHANG C., XU J., ZHAI B., ZHANG B., *Bioresource Technol*., 99 (2008), 8974.
[26] LI Y.L., ZHANG J., ZHU H., YANG F., YANG X.R., *Electrochim. Acta*, 55 (2010), 5123.
[27] WU S.U., ZHAO H.T.N., JU H.X.N., SHI C.G., ZHAO J.W., *Electrochem. Commun*., 8 (2006), 1197.
[28] KARAM P., HALAOUI L.I., *Anal. Chem*., 80 (2008), 5441.
[29] LI X., WANG L., WU Q., CHEN Z., LIN X., *J. Electroanal. Chem*., 735 (2014), 19.
[30] KIVRAK H., ALAL O., ATBAS D., *Electrochim. Acta*, 176 (2015), 497.
[31] SHEN-MING C., VIJAYALAKSHMI V., SELVAKUMAR P., TSE-WEI C., SONADEVI S., SAYEE K.R., BIH-SHOW L., *Sensor. Actuat. B-Chem.*, 252, (2017), 175.
[32] ZHAO D., XU C., *J. Colloid. Interf. Sci*., 447 (2015), 50.
[33] THIRUMALRAJ B., ZHAO D., CHEN S., PALANISAMY S., *J. Colloid. Interf. Sci*., 470 (2016), 117.

Received 2017-04-17
Accepted 2017-08-25